Published in final edited form as:
Chem Res Toxicol. 2009 January ; 22(1): 218–226. doi:10.1021/tx8003714.

Nitrogen Substituent Polarity Influences Dithiocarbamate-Mediated Lipid Oxidation, Nerve Copper Accumulation, and Myelin Injury

Holly L. Valentine[Ψ], **Olga M. Viquez**[Ψ], **Kalyani Amarnath**[Ψ], **Venkataraman Amarnath**[Ψ], **Justin Zyskowski**[§], **Endalkachew N. Kassa**[Ψ,†], and **William M. Valentine**[Ψ,⊥,ζ,*]

Ψ*Department of Pathology, Vanderbilt University Medical Center, 1161 21st Ave. S., Nashville, TN 37232-2561*

⊥*Center in Molecular Toxicology, Vanderbilt University Medical Center, 1161 21st Ave. S., Nashville, TN 37232-2561*

ζ*Center for Molecular Neuroscience, Vanderbilt University Medical Center, 1161 21st Ave. S., Nashville, TN 37232-2561*

§*Diagnostic Center for Population and Animal Health, Michigan State University, 4125 Beaumont Rd, Lansing, MI 48910-8104*

Abstract

Dithiocarbamates have a wide spectrum of applications in industry, agriculture, and medicine, with new applications being investigated. Past studies have suggested that the neurotoxicity of some dithiocarbamates may result from copper accumulation, protein oxidative damage, and lipid oxidation. The polarity of a dithiocarbamate's nitrogen substituents influences the lipophilicity of the copper complexes it generates and thus potentially determines its ability to promote copper accumulation within nerve and induce myelin injury. In the current study, a series of dithiocarbamate-copper complexes differing in their lipophilicity were evaluated for their relative abilities to promote lipid peroxidation determined by malondialdehyde levels generated in an ethyl arachidonate oil-in-water emulsion. In a second component of this study, rats were exposed to either *N*,*N*-diethyldithiocarbamate or sarcosine dithiocarbamate; both generate dithiocarbamate-copper complexes that are lipid and water soluble, respectively. Following the exposures, brain, tibial nerve, spinal cord and liver tissue copper levels were measured by inductively coupled mass spectroscopy to assess the relative abilities of these two dithiocarbamates to promote copper accumulation. Peripheral nerve injury was evaluated using grip strengths, nerve conduction velocities and morphologic changes at the light microscope level. Additionally, the protein expression levels of glutathione transferase alpha and heme-oxygenase-1 in nerve were determined and the quantity of protein carbonyls measured to assess levels of oxidative stress and injury. The data provide evidence that dithiocarbamate-copper complexes are redox active; and that the ability of dithiocarbamate complexes to promote lipid peroxidation is correlated to the lipophilicity of the complex. Consistent with neurotoxicity requiring the formation of a lipid soluble copper complex, significant increases in copper accumulation, oxidative stress and myelin injury were produced by *N*,*N*-diethyldithiocarbamate but not by sarcosine dithiocarbamate.

*Corresponding Author: Department of Pathology, CC3320 MCN VUMC, Nashville, TN 37232-2561, e-mail bill.valentine@vanderbilt.edu, fax 615-343-9825, phone 615-343-5834.
†Currently at University of Missouri, Columbia, MO

Introduction

As a class, dithiocarbamates exhibit a diverse set of chemical properties and biological effects ranging from their cytotoxic and fungicidal properties used in pesticides and soil fumigants to their metal chelating properties used in analytical chemistry and waste management. Dithiocarbamates are also known to modulate the functions of numerous proteins including certain enzymes and transcription factors. The ability of dithiocarbamates to modulate key proteins involved in biological processes including apoptosis, oxidative stress, transcription, and proteasome function has generated interest in these compounds as potential therapeutic agents for assorted conditions including cocaine addiction (1), inflammation (2), viral infections (3), and cancer (4,5). Defining the structural characteristics of dithiocarbamates responsible for beneficial biological effects is key to developing efficacious therapeutic agents; and determining the properties responsible for adverse effects will aid in the safe use of dithiocarbamates in therapeutics.

Previous studies have demonstrated that the polarity of nitrogen substituents on dithiocarbamates greatly influences the stability and solubility as well as the decomposition and metabolic products of a dithiocarbamate in vivo (6–9). The neurotoxic potential of dithiocarbamates has been demonstrated in animal models and observed in human patients. In the peripheral nervous system, both an axonopathy and myelinopathy have been associated with dithiocarbamate exposure in rats (10,11). Investigations on the mechanism of the myelinopathy have reported increased levels of copper and oxidative stress within peripheral nerve, and correlative data have shown a relationship between copper levels and severity of myelin lesions (12,13). More recently elevated copper and lipid peroxidation in nerve were observed to precede the onset of myelin structural lesions detectable by light or electron microscopy (14). The ability of dithiocarbamates to complex copper together with these previous studies has led to the hypothesis that dithiocarbamates form lipophilic complexes with copper that accumulate and promote lipid peroxidation within myelin leading to intramyelinic edema and demyelination. Although elevations in copper and lipid peroxidation precede myelin lesions, the requirement for elevated copper in the observed oxidative stress has not been established. If dithiocarbamate-mediated oxidative stress results from the accumulation of a redox active form of copper, then dithiocarbamate analogues that do not increase copper levels in peripheral nerve could be predicted to not produce myelin injury. Additionally, if the accumulation of copper in nerve results from the generation of lipophilic dithiocarbamate-copper complexes, then dithiocarbamates with polar nitrogen substituents would not be expected to promote copper accumulation in peripheral nerve or produce myelin injury.

In the study presented here, a series of dithiocarbamates (Figure 1) that generate dithiocarbamate-copper complexes differing in their lipophilicity were evaluated for their ability to promote lipid peroxidation in vitro. Lipid peroxidation was assessed through incubation of the dithiocarbamates with Cu^{2+} in an ethyl arachidonate emulsion; and the resulting levels of malondialdehyde (MDA)[1] generated were measured using HPLC after derivatization with diethylthiobarbituric acid (DETBA). Two azo free radical generators differing in their solubility were also incubated with ethyl arachidonate to establish the ability of the system to discriminate between lipid soluble and water soluble free radical generators. As an initial evaluation of the influence of dithiocarbamate nitrogen substituent polarity in vivo, sarcosine dithiocarbamate (SADC), which forms a water soluble copper chelate, and

[1]Abbreviations: MDA, malondialdehyde; TBS, tris buffered saline; GST-α, glutathione transferase alpha; HO-1, heme-oxygenase-1; BSA, bovine serum albumin; DETBA, diethylthiobarbituric acid; SADC, sarcosine dithiocarbamate; DEDC, N,N-diethyldithiocarbamate; AAPH, 2,2'-azobis(2-amidinopropane) dihydrochloride; ABMP, 2,2'-azobis(2-methylpropionitrile); PYDC, pyrrolidine dithiocarbamate, PRODC, proline dithiocarbamate; MEADC, methylacetamide dithiocarbamate; PODC, pyrrolidinone dithiocarbamate; HEDC, *bis*-(2-hydroxyethyl) dithiocarbmamate; Nrf2, NF-E2 p45-related factor; SOD-1, Cu-Zn superoxide dismutase

N,N-diethyldithiocarbamate (DEDC), which forms a lipophilic copper chelate, were administered to rats using conditions previously established for demyelinating injury produced by DEDC (12). Following the exposures, copper levels, myelin lesions, nerve conduction velocities, grip strengths, globin adducts and markers for oxidative stress were evaluated for peripheral nerve.

Experimental Procedures

Materials

2ML4 Alzet® osmotic pumps were obtained from Braintree Scientific (Braintree, MA). Sodium *N,N*-diethyldithiocarbamate, purity 98%, (DEDC) and copper (II) acetate monohydrate were obtained from Alfa Aesar (Ward Hill, MA). Glutaraldehyde was obtained from Electron Microscopy Sciences (Ft. Washington, PA). Fetal bovine serum was obtained from Mediatech Inc. (Herdon, VA). Bovine serum albumin (BSA), 2,2'-azobis(2-amidinopropane) dihydrochloride (AAPH), 2,2'-azobis(2-methylpropionitrile) (ABMP) and pyrogallolsulfonephthalein (pyrogallol red), and ascorbic acid were obtained from Sigma-Aldrich (St. Louis, MO). Dulbecco's PBS (pH=7.4) and ethyl arachidonate were purchased from MP Biomedicals (Irvine, CA). All HPLC grade solvents and DETBA were purchased from Fisher Scientific (Pittsburgh, PA).

Chemicals

The Sodium salts of *bis*-(2-hydroxyethyl) dithiocarbmamate (HEDC), sarcosine dithiocarbamate (SADC), pyrrolidine dithiocarbamate (PYDC), proline dithiocarbamate (PRODC), and the potassium salts of methylacetamide dithiocarbamate (MEADC) and pyrrolidinone dithiocarbamate (PODC) were prepared as previously described (6,15). All were crystallized from ethanol and were found to be identical (with purity greater than 95%) by UV spectroscopy to the reported values (16,17).

In Vitro Dithiocarbamate Incubations and MDA Analysis

An emulsion of ethyl arachidonate in 0.1 M phosphate buffer containing 0.2% SDS (pH 7.4) was prepared by removing the solvent from a 100 mM solution in chloroform (80 μl) and sonicating the residue in the same buffer (1 ml) for 5 min. An aliquot (150 ml) of the suspension was mixed with 1 mM Cu^{2+}, 20 mM ascorbic acid, and phosphate buffer (pH 7.4) alone or with solutions of the seven dithiocarbamates (HEDC, SADC, PYDC, PRODC, MEADC, PODC or DEDC) in the same buffer. The final concentrations were 4 mM ethyl arachidonate, 4 mM ascorbic acid, 0.1 mM Cu^{2+}, dithiocarbamate (0.2 mM) or without the addition of dithiocarbamate (control). The samples were incubated at 37 °C for 2 h and centrifuged at 10,000×*g* for 10 min. Next, 100 μl aliquots of supernatant were mixed with 100 μl 2,6,di-tert-butyl-4-methylphenol (BHT) in ethanol (20mM) and 800 μl of DETBA reagent (18) (100 mg DETBA was dissolved in 10 ml warm ethanol and mixed with 40 ml of 0.125 M phosphate buffer (pH 3.0)) and incubated at 95 °C for 1 h. After cooling, the solutions were purified by passing through 1 ml Supelclean LC-18 SPE cartridges (Supelco, Inc., Bellefonte, PA) and eluted with methanol and dried. The residue was reconstituted with 100 μl of a 1:1 mix of eluent A and B. Eluent A was 10 % acetonitrile with 0.1% triethanolamine and eluent B was 100% acetonitrile. After filtration through 0.22μm SPIN-X filters (Corning Inc., Corning, NY), the samples were analyzed using a LichroCART 125 × 4 mm Lichrosphere 100 RP-18 (5 μm) column (EM Science, Gibbstown, NJ) running at 1 ml/min. The elution profile was 100% A going to 90% B in 7 min, holding for 5 min, and returning to A in 1 min. A Shimadzu LC-10AD pump connected to a SIL-10AD autosampler and SPD-10A uv/vis detector controlled by a SLC-10A controller and EZStart 7.4 software was used for the analysis. Under these conditions the MDA adduct was detected at 530 nm and eluted at 8.5 min. Standard solutions of 1,1,3,3-

tetramethyoxypropane (TMP), precursor to MDA, in a 1:1 mixture of ethanol and water were made and reacted with DETBA reagent for generation of a MDA standard curve.

Incubations with Azo Free Radical Generators

MDA analysis and incubation conditions identical to those used for the dithiocarbamates were used for incubations with 2,2'-azobis(2-methylpropionitrile) (ABMP) or 2,2'-azobis(2-amidinopropane) dihydrochloride (AAPH) except that copper acetate and ascorbic acid were not added. The concentrations of AAPH and ABMP were both 1.6 mM and the incubations were performed in triplicate. The decomposition rates of AAPH and ABMP at 37°C were determined using a previously published method based upon the loss of absorbance at 539 nm of pyrogallol red over a 2 h period (19). Spontaneous loss of dye was monitored identically in the absence of AAPH or ABMP.

Animal Exposures and Biological Methods

All treatments and procedures using animals were conducted in accordance with the National Institutes of Health *Guide for the Care and Use of Laboratory Animals* and approved by the Institutional Animal Care and Use Committee of Vanderbilt University. Eighteen adult male Sprague-Dawley rats were obtained from Harlan Bioproducts (Indianapolis, IN) and caged at Vanderbilt University animal facilities in a temperature controlled room (21–22 °C) with a 12 h light–dark cycle, supplied with Purina Lab Diet 5001, a segment of 4 inch diameter PVC tubing for environmental enrichment, and water *ad libitum*. After an 8-day acclimatization period, 12 animals were exposed to either DEDC (n=6) or SADC (n=6) at 0.3 mmol/kg/day for 8 weeks using 2mL, 4-week Alzet® osmotic pumps (Braintree Scientific, Braintree, MA) surgically implanted in the abdomen under anesthesia (100 mg/Kg ketamine with 8 mg/Kg xylazine ip). The osmotic pumps were replaced after 4 weeks to extend the exposure period to 8 weeks. Six additional animals served as controls and did not receive pumps. DEDC (98% purity) and SADC (> 95% purity) were delivered as an aqueous solution, the concentration of which was determined from the UV absorbance at 282 nm (DEDC, ε= 13,000 $M^{-1}cm^{-1}$), and at 283.5 nm (SADC, ε= 11,950 $M^{-1}cm^{-1}$). SADC and DEDC were sterilized prior to filling the pumps by filtering through a 0.22 μm syringe filter. The average starting body wt of all 18 animals was 311 ± 1.9 g (SE), and all animals were weighed twice a week during the 8-week exposure.

Neuromuscular function was assessed at the end of the exposure period for all groups by measuring hind-limb grip strength and nerve conduction velocity (NCV). Grip strength measurement was accomplished using a DFIS 10 digital force gauge (John Chantillon & Sons, Greensboro, NC) (20). The peak compression achieved by each animal on 3 successive trials was recorded and expressed as the average ± SE for each exposure and control group. NCV studies were performed on anesthetized rats (100 mg/Kg Ketamine with 8 mg/Kg Xylazine ip). Temperature was maintained using radiant heat and a Deltaphase isothermal pad (Braintree Scientific, Inc, Braintree, MA) and monitored with a skin temperature probe applied to the ventral surface of the proximal tail. The TECA Synergy N2 System (Viasys Healthcare, Madison, WI) connected to a pre-configured notebook computer and Teca-Synergy V 12.2 Software was used to measure and record NCV. Sciatic-tibial motor NCV was determined by placing a stimulating cathode electrode proximally at the sciatic notch and distally near the posterior tibial nerve on the medial side of the tarsus. Supramaximal electrical stimulation was applied using pulses of 20 μsec at a frequency of 0.2 Hz, and the evoked compound action potential measured three times for each site in the lumbrical or interosseous muscles on the plantar surface of the hind foot using two monopolar recording electrodes. Latency times for each site were determined by measuring the time between stimulus and the peak of the evoked compound action potential. Three latency time measurements for each site were averaged to calculate the individual animal's latency for each site. Maximum motor nerve conduction

velocity was calculated by taking the distance (cm) between the 2 stimulating sites measured on the skin with the use of calipers and dividing by the difference between the sciatic and tarsal latency time (s) and multiplying by 10. The 6 individual rat NCV measurements were averaged and SE calculated for each exposed and control group.

After NCV measurements were performed, control and exposed animals were exsanguinated by cardiac puncture. Whole blood (1 mL) was placed into heparinized vials for globin isolation. The left sciatic nerve was removed and cut in half and immediately frozen in liquid nitrogen and stored at −80 °C for protein isolation. The right sciatic nerve was immersed in 4% glutaraldehyde in 0.1 M PBS (pH 7.4) for histopathology. A section of the liver, half of the brain, cut sagittally, sections of proximal spinal cord, and both posterior tibial nerves were immersed in 4% glutaraldehyde in 0.1M PBS (pH 7.4), and stored at 4°C for metal analysis.

Analysis of Tissue Metal Levels

Tissue sections of brain, spinal cord, and liver and both tibial nerves were analyzed by inductively coupled plasma mass spectrometry (ICP-MS) at the Diagnostic Center for Population and Animal Health at Michigan State University (East Lansing, MI). Brain tissue samples for ICP-MS were approximately 2 mm mid-sagittal slices; liver sections were approximately $1cm^3$ pieces of tissue; tibial nerve tissues were approximately 15- to 20-mm lengths of both nerves; spinal cord sections were approximately 15 mm in length of the proximal region. Values were reported as ppm per dry wt of tissue.

RP/HPLC Analysis of Globin

Globin isolation and analysis to quantify adduct formation was performed as previously described (12,21). Dried globin was solubilized with 0.1% trifluoroacetic acid (TFA) to produce a solution for HPLC analysis. Globin chains were separated by RP-HPLC on a Phenomenex Jupiter 5 μm C_4 column (150 × 2 mm) using a Waters 2690 liquid chromatograph after adjusting sample concentration to a UV absorption of 1.0 ± 0.2 at 280 nm. Globins were separated using a linear gradient from 56% solvent A and 44% solvent B to 30% solvent A and 70% solvent B over 30 min followed by a linear gradient to 100% solvent B over 10 min. Solvent A was 20:80:0.1 acetonitrile/water/TFA, and solvent B was 60:40:0.08 acetonitrile/water/TFA. The elution of globin peaks was monitored by their UV absorption at 220 nm using a Waters 996 photodiode array detector.

Protein Extraction and Quantification

Approximately 10 mg of frozen sciatic nerve was powdered in a mortar and pestle in liquid nitrogen. Total sciatic nerve proteins were extracted using 0.4 mL chilled TNE buffer (2 mM EDTA, 150 mM NaCl, 50 mM Tris-base, 2 mM DTT, and NP-40 (1%, v/v)), containing protease inhibitors (P-2714 Sigma-Aldrich, St. Louis, MO, and 80-6501-23 protease inhibitor mix, Amersham Biosciences, Piscataway, NJ) and phosphatase inhibitors (P-2850 and P-5726 Sigma-Aldrich). The homogenate was sonicated in ice/water for 3 min and centrifuged at 40,485×g for 20 min at 4 °C. The supernatant was collected and stored at −80 °C. Protein concentration in the supernatant of the nerve samples was measured by a modified Bradford method (22) using BSA as the standard.

Determination of Protein Carbonyls

Protein carbonyl content of nerve samples and standards were determined by the fluoresceinamine-cyanoborohydride method using immunochemical detection as previously described (23). Briefly, 25 μg aliquots of protein were treated with fluoresceinamine (12 μL of 0.25 M) and sodium cyanoborohydride (10 μL of 0.4 M) for 1 h at 37°C. Next, protein was precipitated at room temperature with methanol:water:chloroform (4:3:1, v/v). Precipitates

were washed 5 times with acidified ethanol:ethyl acetate (1:1) for 5 min at 37°C followed by centrifugation (15,000×g, 9 min) and then solubilized in 250 μL sodium hydroxide (0.1 N) for 15 min at 37°C. Treated proteins (controls, SADC or DEDC-exposed) were bound to Immobilon-P membranes (Millipore, MA, polyvinylidine difluoride (PVDF) membranes) using the Bio-Dot® Blot apparatus (BioRad, CA). Four replicates per sample containing approximately 0.4 μg of sciatic nerve protein per well were loaded. Protein carbonyls were detected using the CDP-Star Universal Alkaline Phosphatase kit (Sigma-Aldrich) following the manufacturer's instructions. Kodak X-Omat Blue XB-1 film was exposed to the treated membrane at room temperature for 20 min. For quantification, films were scanned with a GS-700 densitometer (Bio-Rad, Hercules, CA) and analyzed using Quantity One® 1-D Analysis Program version 4.1 (Bio-Rad). The protein carbonyl content of samples was determined from a standard curve generated using oxidized BSA for which carbonyl content was determined spectrophotometrically (ε=86,000 $M^{-1}cm^{-1}$ at 490 nm) using a Shimadzu UV-2401 PC. Oxidized BSA standards were prepared by incubating 10 mg of BSA dissolved in 1 ml of 20 mM Tris HCl (pH 7.4) with 100 mM Fe^{2+} and 100 mM hydrogen peroxide, at room temperature for 1 h. Reduced BSA was used as a negative control and was prepared by mixing oxidized-BSA (10 mg/mL) with 5 mg of sodium borohydride for 30 min at 37°C. The quantity of nerve protein bound to the PVDF membrane was determined using the MemCode™ Reversible Protein Stain Kit for PVDF membranes (Pierce, Rockford, IL).

Western Blotting for Heme-Oxygenase-1 and Glutathione Transferase-α

Equal amounts of sciatic nerve protein (20 μg) were separated by SDS-PAGE (NuPAGE® 4–12% bis-tris gel, Invitrogen, Carlsbad, CA) along with molecular weight markers (Novex®Sharp Pre-Stained Protein Standards (MW 3.5–260 kDa), MagicMark™ XP Western Standard, Invitrogen Carlsbad, CA). Separated proteins were electrophoretically transferred onto an Immobilon-P membrane using an XCell II™ Blot Module (Invitrogen, Carlsbad, CA). Nonspecific binding sites were blocked in blocking buffer (5% nonfat powdered skim milk in tris buffered saline, pH 7.4, containing 0.1% Tween-20 (TBST) at room temperature for 1 h. Membranes were then incubated with primary antibodies against heme-oxygenase-1(HO-1) (OSA-111, mouse anti-heme-oxygenase-1, Stressgen, Ann Arbor, MI, dilution 1:1,000), or glutathione transferase-α (GST-α) (GSTA11: rabbit anti-GST-α, Alpha Diagnostic, San Antonio, TX, dilution 1:2,000) overnight at 4 °C. Concurrently, with the anti-GST-α or anti-HO-1, membranes were also incubated with primary anti-actin antibody (A-2066, rabbit anti-actin, Sigma, St. Louis, MO, dilution 1:5,000). After rinsing with TBST, the membranes were incubated at room temperature for 1 h with donkey anti-mouse (SC-2314, Santa Cruz Biotechnology, Santa Cruz, CA, dilution 1:10,000) or anti-rabbit peroxidase conjugated secondary antibody (A-8275, Sigma, St. Louis, MO, dilution 1:10,000). Following three 10 min washes in TBST, the membranes were incubated with Western Lightning Chemiluminescence Reagent Plus substrate (Perkin-Elmer LAS, Inc., Boston, MA), and exposed to Kodak X-Omat Blue XB-1 film. The presence of GST-α (MW = 25 kDa) was confirmed by comparing the migration of positive control GST (rat liver, Sigma, St. Louis, MO) to the molecular weight standard. The presence of HO-1 (MW = 32 kDa) and actin (MW = 42 kDa) was confirmed by comparison to the molecular weight standard. For quantification, films were scanned with a GS-700 densitometer (Bio-Rad) and analyzed using Quantity One 1-D Analysis Program version 4.1 (Bio-Rad). Normalization of each protein of interest was performed for each sample relative to its corresponding actin value.

Preparation of Tissue for Morphology

Dissected sciatic nerves from control, DEDC and SADC-exposed animals were immersed in 4% glutaraldehyde in 0.1M Dulbecco's PBS buffer (pH 7.4) and held at 4°C. For morphology, sciatic nerve sections were post-fixed with osmium tetroxide and embedded in Low-Viscosity Spurr Embedding Media (Electron Microscopy Sciences, Fort Washington, PA). Thick

sections (600 nm) were cut and stained with toluidine blue. The thick sections of peripheral nerve were evaluated by light microscopy on an Olympus BX41 microscope equipped with an Optronics Microfire digital camera. One cross section of sciatic nerve was examined per animal and the total number of lesions counted. The lesions quantified were: degenerated axons, axons with thin myelin (*g* ratio greater than 0.7 (axon/axon with myelin diameter)), intramyelinic edema, and demyelinated axons. The surface area of the sciatic nerve was quantified using Photoshop with Fovea Pro 4 plug-ins and the number of lesions/mm^2 calculated for each section.

Statistical Analysis

One-way analysis of variance (ANOVA), Tukey–Kramer's Multiple Comparisons Test, and Chi-Square Test for Trend were performed using InStat 3.0 (Graphpad Software, Inc.). Lesion counts were square root transformed to normalize their distribution and equalize variances prior to statistical comparisons by ANOVA and Tukey-Kramer's Multiple Comparisons Test. Statistical significance was taken to be $p < 0.05$ unless otherwise noted. Linear fit was performed using KaleidaGraph (version 3.6, Synergy Software).

Results

In Vitro Dithiocarbamate Incubations

The amount of MDA produced from the incubation of each dithiocarbamate with ethyl arachidonate compared to the amount of MDA generated without the addition of dithiocarbamate (control) is presented in Figure 2A. A significant increase in MDA (pmol ± SE) was seen for PRODC (18.46 ± 0.73), MEADC (46.98 ± 3.69), DEDC (66.05 ± 1.76), PODC (74.07 ± 4.9) and PYDC (87.56 ± 2.5) relative to the control (6.83 ± 1.00), whereas no significant increase was seen for SADC (4.37 ± 0.46) or HEDC (4.92 ± 0.24). As seen in Figure 2B, the levels of MDA generated were positively correlated ($p<0.05$, $r^2 = 0.63$) to the octanol/water partition coefficients (log P_{ow}) of the dithiocarbamate-copper complexes calculated using ChemBioDraw Version II (CambridgeSoft).

Incubations with Free Radical Generators

The more lipophilic free radical generator, ABMP (log $P_{ow} = 1.2$), produced significantly greater levels of MDA relative to AAPH (log $P_{ow} = 1.0$) or the control (Figure 2C). No significant differences in MDA generation were observed between the control and APPH incubations. The relative rates of decomposition based upon loss of dye absorbance at 539 nm in Abs/min (SE) were: 2.56×10^{-3} (1.3×10^{-5}) and 1.06×10^{-3} (7.1×10^{5}) and for AAPH and ABMP, respectively.

Body Weights, Grip Strengths, and Nerve Conduction Velocity Measurements

The average weight gain (g ± SE, n=6 all groups) of the DEDC-exposed animals was significantly decreased (55.3 ± 8.6, $p < 0.01$) as compared to the SADC (110.0 ± 3.1) and control (107.7 ± 7.3) groups.

Hind limb grip strength data and NCV values for all exposure groups are presented in Figure 3A and 3B, respectively. Hind limb grip strength and NCV values were both significantly decreased in the animals given DEDC for 8 weeks relative to the SADC-exposed and control animals and no significant decrease was seen between the SADC and control groups.

Analysis of Tissue Metal Levels

Copper levels in brain, spinal cord, tibial nerve, and liver in the DEDC-exposed group were significantly elevated over the control and SADC-exposed groups (Figure 4). Of the other

metals analyzed (zinc, iron, manganese, selenium, arsenic, molybdenum) by ICP-MS, the only significant difference found was an elevation of zinc content in the liver from DEDC-exposed animals. Zinc in liver (ppm ± SE) was measured at 120.9 ± 5.9 in DEDC-exposed animals compared to 86.8 ± 1.6 in SADC-exposed animals and 83.3 ± 5.0 in controls ($p < 0.01$ for DEDC group as compared to both SADC and control groups, n=6 for all groups).

Globin Analysis

Globin preparations from all animals exposed to DEDC contained an additional HPLC peak that was not observed in globin preparations from control animals or SADC-exposed animals. Earlier work demonstrated that this additional peak is produced by carbamylation of Cys-125 of a β-globin chain by a metabolite of DEDC to produce *S*-(diethylaminocarbonyl)-cysteine adducts on Cys-125 and is correlated to dose level (21,24). At the end of the 8 weeks, the mean levels ± SE of modified β-globin expressed as a percent of total peak area for the DEDC-exposed group was 16.0 ± 0.6%. No analogous late-eluting peak was detected in globin samples obtained from SADC treated rats.

Assessment of Oxidative Stress and Injury

Western blots of sciatic nerve proteins demonstrated significant increases in GST-α and HO-1 in nerve from DEDC-exposed animals relative to SADC-exposed and control animals (Figure 5A, B). Dot-blot and subsequent immunochemical detection of protein carbonyls demonstrated a significant increase in carbonyl content in sciatic nerve proteins isolated from rats exposed to DEDC relative to that of control and SADC- exposed rats (Figure 5C).

Peripheral Nerve Morphology

Representative sections of sciatic nerve obtained from controls and animals exposed to DEDC or SADC are shown at the light microscope level in Figure 6 and demonstrate the lesions quantified in Table 1. Axons undergoing degeneration were observed in all animals from each of the three groups. There was a significant increase in the severity of axonal degeneration seen in the DEDC group relative to the SADC and control groups and in the SADC group relative to the controls (Table 1). Myelin lesions were only observed in sections prepared from the DEDC-exposed animals. The incidence and severity of demyelination and the incidence of intramyelinic edema were significantly increased in the DEDC group relative to the other two treatment groups. In addition, axonal regeneration was evidenced by the presence of axonal sprouts seen in one of the sections of the six animals exposed to DEDC.

Discussion

The present study used an in vitro system to evaluate the ability of dithiocarbamates to complex copper and promote lipid peroxidation as a putative mechanism for dithiocarbamate-mediated copper accumulation and oxidative stress in peripheral nerve. The ability of this system to discriminate based upon solubility properties of the initiator was verified using two azo free radical generators differing in their octanol water partition coefficients, AAPH and ABMP. Seven dithiocarbamates varying in the polarity of their nitrogen substituents were examined. Five of the seven produced significantly elevated levels of MDA relative to copper alone and the levels of MDA were significantly correlated to the lipophilicity of the dithiocarbamate copper complex. This suggests that dithiocarbamates can facilitate transport of the relatively water-soluble copper ion into the hydrophobic region of the emulsion resulting in the generation of reactive oxygen species in closer proximity to the unsaturated carbon chain of ethyl arachidonate than in the absence of dithiocarbamate (Scheme 1). Slightly greater levels of MDA were generated by PYDC and PODC relative to the more lipophilic DEDC and this may have reflected the greater stability of the cyclic dithiocarbamates relative to DEDC (25). Less clear though was the low level of MDA produced by HEDC that was not predicted by its

partition coefficient. Given that HEDC is an effective chelator of Cu^{2+} and used for this purpose analytically (26), an inability to bind Cu^{2+} does not appear responsible for this result. Alternatively, the HEDC complex may be less lipid soluble than predicted by the calculated partition coefficient or less redox active than the other complexes. Unfortunately, the contribution from differences in copper affinity or redox potential for the individual complexes cannot be quantitatively compared from the present experiments. However, the high affinity for Cu^{2+} of the analogs used here and dithiocarbamates in general (27–29) and the observed capacity to enhance lipid peroxidation over copper alone suggest that dithiocarbamates that form lipophilic copper complexes can facilitate copper-mediated lipid peroxidation.

The second component of this study extended the in vitro experiments to examine the influence of nitrogen substituent polarity on copper accumulation, oxidative stress and neurotoxicity in vivo using SADC and DEDC. It was determined that DEDC produced significant changes in all of these parameters whereas SADC did not. DEDC significantly increased total copper in brain, peripheral nerve and liver to similar levels reported in previous studies (12,14). In addition, significantly elevated levels of copper that were intermediate between those in nerve and brain were observed for spinal cord in the current investigation. These data suggest that the nitrogen substituents' polarity is a determinant of a dithiocarbamate's ability to promote copper accumulation within the nervous system. This relationship may be applicable to other metals as well in that DEDC is also more effective than SADC in distributing cadmium to the brain in cadmium exposed experimental animals (30).

Among metals present within biological systems, DEDC binds copper with the greatest affinity (29); and DEDC has been shown to inhibit SOD-1 through removal of its copper co-factor in vivo(31). In the current study, no significant changes in the levels of metals other than copper were observed in the nervous system. However, zinc was significantly elevated in the liver of DEDC-exposed animals over the SADC and control animals. The underlying mechanism and biological significance for this elevation of liver zinc is currently undetermined. It is possible that this may be related to the ability of DEDC to form a lipophilic yet less stable DEDC-zinc complex (29). A previous study also found a trend toward elevation of zinc in the liver of DEDC treated rats (12), however, no treatment related lesions in the liver or elevations in aspartate amino transferase were found in any of the animals examined. Previous studies have demonstrated that elevations in lipid peroxidation and protein expression levels of antioxidant enzymes in peripheral nerve accompanied DEDC administration (14,32). Increased expression of glutathione transferase isoforms has been detected in nerve by proteomic analyses; and the observation that elevations of peripheral nerve MDA and F_2-isoprostanes preceded the onset of lesions suggested that lipid peroxidation could contribute to the development of myelin lesions. In the present study, two proteins, GST-α and HO-1, whose expression is at least partly regulated by the binding of Nrf2 to the antioxidant response element, were used as indices of oxidative stress (33). GST-α is important in detoxifying 4-hydroxynonenal and has been demonstrated to be up regulated in conditions producing elevation in lipid peroxidation (34). Protein carbonyls can be elevated from metal catalyzed oxidation (35) and from lipid peroxidation products, including 4-hydroxynonenal, that add to nucleophilic sites of proteins; and both of these processes can generate aldehydes detectable by the fluoresceinamine assay used here. Thus the results obtained in vivo for SADC and DEDC appear consistent with only DEDC causing oxidative stress and protein oxidative injury in nerve.

Because the primary function of myelin is to increase the velocity of action potential conduction, the measurement of maximal nerve conduction velocities provide a good in vivo assessment of myelin integrity of peripheral nerve (36). Hind limb grip strength also furnishes a relatively objective assessment of neuromuscular function with the potential to identify deficits prior to the onset of structural lesions (37). In the present study, significant decreases

in both these parameters as well as significant increases in myelin lesions only resulted for DEDC in conjunction with elevated tissue copper and oxidative stress.

Evidence for the ability of dithiocarbamates to increase intracellular levels of redox active copper via diffusion through the cell membrane in vitro has been presented previously and the cytotoxicity of PYDC and Cu^{2+} was three orders of magnitude greater together than for either Cu^{2+} or PYDC alone. Cell death in those studies was attributed to occur through apoptosis mediated by oxidative stress (38,39). Polarity has also been investigated for modifying the ability of dithiocarbamates to penetrate the plant cuticle and produce intracellular effects in herbicidal applications (28). Analogous to a cells plasma membrane, a diffusion barrier separates most of the central and peripheral nervous system from the circulatory system. Thus, the transformation of the water-soluble ionic dithiocarbamate to a lipophilic dithiocarbamate copper complex could facilitate diffusion across the blood brain or blood nerve barrier. Once inside the nervous system, the lipophilic complex may partition into myelin with its high concentration of polyunsaturated fatty acids. This would sequester copper in the nervous system, contribute to its accumulation with continuing exposure, and serve to concentrate the copper in the site of primary lesion development. To evaluate this possibility, further experiments are required to localize and characterize the excess copper within the nervous system.

The in vitro data in the current study support the ability of dithiocarbamates to form redox active complexes that according to their solubility properties can partition into lipid compartments and initiate lipid peroxidation. The contrast observed in the neurotoxicity of SADC and DEDC suggests that the solubility properties of the associated dithiocarbamate-copper complex may also influence the potential of a dithiocarbamate to promote copper accumulation, oxidative stress, and myelin injury in vivo as well. An interpretation consistent with this and previous studies is that the key-initiating event is the accumulation of redox active copper within nerve. An unanswered central question to this interpretation is whether the bis-dithiocarbamate-Cu^{2+} complexes generated here in vitro are generated in vivo and transport copper into nerve, resulting in its accumulation. Relative to the controlled conditions used here for the incubations, there are many more possibilities in vivo including complexation of Cu^{2+} between a dithiocarbamate and other copper binding molecules, e.g. cysteine. Further studies are required to determine the source, chemical species, oxidation state and location of the excess copper within nerve to advance our understanding of the role and nature of copper dysregulation in dithiocarbamate myelinopathy. Although studies have provided evidence that dithiocarbamate-derived thiocarbonyl cysteine adducts do not contribute to dithiocarbamate-mediated myelinopathy (11) the contribution of other recognized biological affects of dithiocarbamates, e.g., proteasome, Nfκβ and cuproenzyme inhibition (40), to dithiocarbamate induced neurotoxicity have not been adequately evaluated yet. Such studies will help to formulate structure-activity relationships that can be used to make mechanism-based risk assessments, characterize and predict the long term effects of low level dithiocarbamate exposures, and help to design safer and more efficacious dithiocarbamates for therapeutic and pesticide applications.

Acknowledgment

This work was supported by NIEHS Grant ES06387 and P30 ES00267. Experiments were performed in part through the use of the VUMC Research EM Resource (sponsored by NIH Grants DK20539 and DK58404).

References

1. Sofuoglu M, Kosten TR. Novel approaches to the treatment of cocaine addiction. CNS Drugs 2005;19:13–25. [PubMed: 15651902]

2. Fang IM, Yang CH, Lin CP, Yang CM, Chen MS. Effects of pyrrolidine dithiocarbamate, an NF-kappaB inhibitor, on cytokine expression and ocular inflammation in experimental autoimmune anterior uveitis. J. Ocul. Pharmacol. Ther 2005;21:95–106. [PubMed: 15857275]
3. Si X, McManus BM, Zhang J, Yuan J, Cheung C, Esfandiarei M, Suarez A, Morgan A, Luo H. Pyrrolidine dithiocarbamate reduces coxsackievirus B3 replication through inhibition of the ubiquitin-proteasome pathway. J. Virol 2005;79:8014–8023. [PubMed: 15956547]
4. Bach SP, Chinery R, O'Dwyer ST, Potten CS, Coffey RJ, Watson AJ. Pyrrolidinedithiocarbamate increases the therapeutic index of 5-fluorouracil in a mouse model. Gastroenterology 2000;118:81–89. [PubMed: 10611156]
5. Daniel KG, Chen D, Orlu S, Cui QC, Miller FR, Dou QP. Clioquinol and pyrrolidine dithiocarbamate complex with copper to form proteasome inhibitors and apoptosis inducers in human breast cancer cells. Breast Cancer Res 2005;7:R897–R908. [PubMed: 16280039]
6. Amarnath V, Amarnath K, Valentine WM. Mechanism of decomposition of *N,N*-dialkyl dithiocarbamates. Curr. Topics Toxicol 2007;4:39–44.
7. Garcia JI, Humeres E. Mechanisms of acid decomposition of dithiocarbamates. 4. Theoretical calculations on the water-catalyzed reaction. J. Org. Chem 2002;67:2755–2761. [PubMed: 11975525]
8. Humeres E, Debacher NA, Franco JD, Lee BS, Martendal A. Mechanisms of acid decomposition of dithiocarbamates. 3. Aryldithiocarbamates and the torsional effect. J. Org. Chem 2002;67:3662–3667. [PubMed: 12027677]
9. Humeres E, Debacher NA, Sierra MM. Mechanisms of Acid Decomposition of Dithiocarbamates. 2. Efficiency of the Intramolecular General Acid Catalysis. J. Org. Chem 1999;64:1807–1813. [PubMed: 11674268]
10. Johnson DJ, Graham DG, Amarnath V, Amarnath K, Valentine WM. Release of carbon disulfide is a contributing mechanism in the axonopathy produced by N,N-diethyldithiocarbamate. Toxicol. Appl. Pharmacol 1998;148:288–296. [PubMed: 9473537]
11. Tonkin EG, Valentine HL, Zimmerman LJ, Valentine WM. Parenteral N,N-diethyldithiocarbamate produces segmental demyelination in the rat that is not dependent on cysteine carbamylation. Toxicol. Appl. Pharmacol 2003;189:139–150. [PubMed: 12781632]
12. Tonkin EG, Valentine HL, Milatovic DM, Valentine WM. N,N-diethyldithiocarbamate produces copper accumulation, lipid peroxidation, and myelin injury in rat peripheral nerve. Toxicol. Sci 2004;81:160–171. [PubMed: 15187237]
13. Valentine HL, Amarnath K, Amarnath V, Valentine WM. Dietary copper enhances the peripheral myelinopathy produced by oral pyrrolidine dithiocarbamate. Toxicol. Sci 2006;89:485–494. [PubMed: 16291825]
14. Viquez OM, Valentine HL, Amarnath K, Milatovic D, Valentine WM. Copper accumulation and lipid oxidation precede inflammation and myelin lesions in N,N-diethyldithiocarbamate peripheral myelinopathy. Toxicol. Appl. Pharmacol 2008;229:77–85. [PubMed: 18284930]
15. Takeshima T, Ikeda M, Yokoyama M, Fukada N, Muraoka M. Reaction of carbon disulfide with cyclic amides and related compounds. Free N-acyl- and N-carbamoyl-dithiocarbamic acids. J. Chem. Soc., Perkin 1979;1:692–695.
16. Beaty JA, Jones MM, Wilson DJ, Ma L. An in vitro model for the in vivo mobilization of cadmium by chelating agents using 113Cd-NMR spectroscopy. Chem. Res. Toxicol 1992;5:568–575. [PubMed: 1391624]
17. Jones MM, Singh PK, James SG, Gale GR, Atkins LM, Smith AB. Structure-activity relationships for in vivo cadmium mobilization by dithiocarbamates derived from lactose and maltotriose. Chem. Res. Toxicol 1991;4:692–698. [PubMed: 1807453]
18. Guichardant M, Valette-Talbi L, Cavadini C, Crozier G, Berger M. Malondialdehyde measurement in urine. J. Chromatogr. B Biomed. Appl 1994;655:112–116. [PubMed: 8061818]
19. Yoshida Y, Itoh N, Saito Y, Hayakawa M, Niki E. Application of water-soluble radical initiator, 2,2'-azobis[2-(2-imidazolin-2-yl)propane] dihydrochloride, to a study of oxidative stress. Free Radical Res 2004;38:375–384. [PubMed: 15190934]
20. Meyer OA, Tilson HA, Byrd WC, Riley MT. A method for the routine assessment of fore- and hindlimb grip strength of rats and mice. Neurobehav. Toxicol 1979;1:233–236. [PubMed: 551317]

21. Erve JC, Jensen ON, Valentine HS, Amarnath V, Valentine WM. Disulfiram generates a stable N,N-diethylcarbamoyl adduct on Cys-125 of rat hemoglobin beta-chains in vivo. Chem. Res. Toxicol 2000;13:237–244. [PubMed: 10775322]
22. Ramagli LS. Quantifying protein in 2-D PAGE solubilization buffers. Methods Mol. Biol 1999;112:99–103. [PubMed: 10027233]
23. Levine RL, Garland D, Oliver CN, Amici A, Climent I, Lenz AG, Ahn BW, Shaltiel S, Stadtman ER. Determination of carbonyl content in oxidatively modified proteins. Methods Enzymol 1990;186:464–478. [PubMed: 1978225]
24. Tonkin EG, Erve JC, Valentine WM. Disulfiram produces a non-carbon disulfide-dependent schwannopathy in the rat. J. Neuropathol. Exp. Neurol 2000;59:786–797. [PubMed: 11005259]
25. Topping RJ, Jones MM. Optimal dithiocarbamate structure for immunomodulator action. Med. Hypotheses 1988;27:55–57. [PubMed: 2849708]
26. King J, Fritz JS. Concentration of metal ions by complexation with sodium bis(2-hydroxyethyl) dithiocarbamate and sorption on XAD-4 resin. Anal. Chem 1985;57:1016–1020.
27. Yamuna K, Ramana VV, Emmanuel KA, Saraswati K. Stability constants of metal complexes of dithiocarbamates. Asian J. Chem 1992;4:387–389.
28. Rogachev I, Kampel V, Gusis V, Cohen N, Gressel J, Warshawasky A. Synthesis, properties, and use of copper-chelating amphiphilic dithiocarbamates as synergists of oxidant-generating herbicides. Pestic. Biochem. Physiol. FIELD Full Journal Title:Pesticide Biochemistry and Physiology 1998;60:133–145.
29. Gessner, PK.; Gessner, T. Disulfiram and its metabolite Diethyldithiocarbamate: Pharmacology and status in the treatment of alcoholism, HIV infections, AIDS and heavy metal toxicity. London: Chapman & Hall; 1992. p. 7-12.
30. Jones SG, Jones MM. Structure-activity relationships among dithiocarbamate antidotes for acute cadmium chloride intoxication. Env. Health Perspec 1984;54:285–290.
31. Heikkila RE, Cabbat FS, Cohen G. In vivo inhibition of superoxide dismutase in mice by diethyldithiocarbamate. J. Biol. Chem 1976;251:2182–2185. [PubMed: 5443]
32. Viquez OM, Valentine HL, Friedman DB, Olson SJ, Valentine WM. Peripheral nerve protein expression and carbonyl content in N,N-diethlydithiocarbamate myelinopathy. Chem. Res. Toxicol 2007;20:370–379. [PubMed: 17323979]
33. Nguyen T, Sherratt PJ, Pickett CB. Regulatory mechanisms controlling gene expression mediated by the antioxidant response element. Ann. Rev. Pharmacol. Toxicol 2003;43:233–260. [PubMed: 12359864]
34. Awasthi YC, Ansari GA, Awasthi S. Regulation of 4-hydroxynonenal mediated signaling by glutathione S-transferases. Methods Enzymol 2005;401:379–407. [PubMed: 16399399]
35. Requena JR, Chao CC, Levine RL, Stadtman ER. Glutamic and aminoadipic semialdehydes are the main carbonyl products of metal-catalyzed oxidation of proteins. Proc. Natl. Acad. Sci. U S A 2001;98:69–74. [PubMed: 11120890]
36. Kimura, J. Nerve conduction and needle electromyography. Vol. Fourth Edition ed. Vol. Vol. 1. Philadelphia: Elsevier Inc; 2005.
37. Moser VC, Phillips PM, Morgan DL, Sills RC. Carbon disulfide neurotoxicity in rats: VII. Behavioral evaluations using a functional observational battery. Neurotoxicol 1998;19:147–157.
38. Chen SH, Liu SH, Liang YC, Lin JK, Lin-Shiau SY. Death signaling pathway induced by pyrrolidine dithiocarbamate-Cu(2+) complex in the cultured rat cortical astrocytes. Glia 2000;31:249–261. [PubMed: 10941151]
39. Nobel CI, Kimland M, Lind B, Orrenius S, Slater AF. Dithiocarbamates induce apoptosis in thymocytes by raising the intracellular level of redox-active copper. J. Biol. Chem 1995;270:26202–26208. [PubMed: 7592825]
40. Cvek B, Dvorak Z. Targeting of nuclear factor-kappaB and proteasome by dithiocarbamate complexes with metals. Curr. Pharm. Design 2007;13:3155–3167.

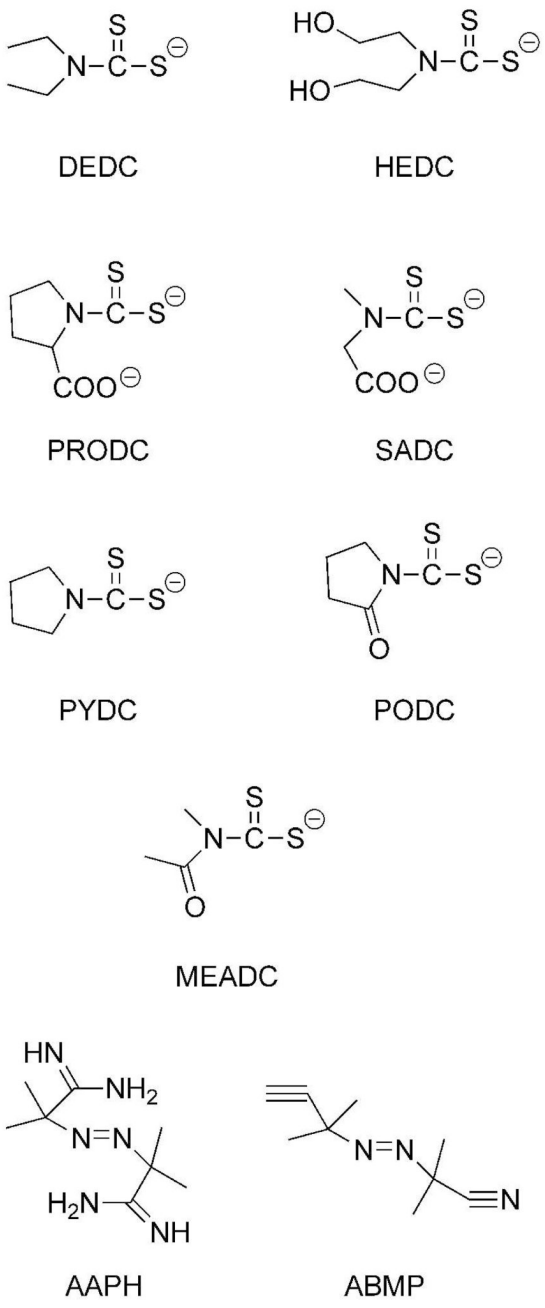

Figure 1.
Structures of dithiocarbamates and azo free radical generators used for in vitro incubations and animal exposures.

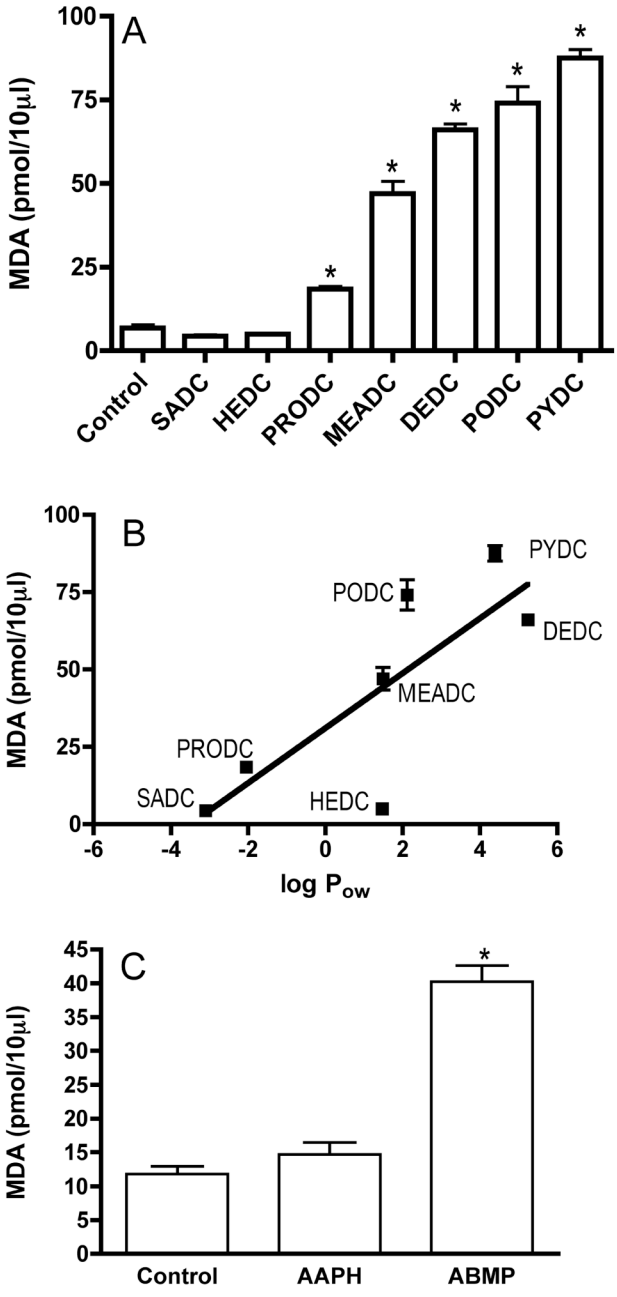

Figure 2.

Amount of MDA generated by the in vitro incubation of dithiocarbamates or azo free radical generators with ethyl arachidonate. (A) Values obtained for dithiocarbamates. (B) MDA generated as a function of the octanol water partition coefficient. (C) Values obtained for azo free radical generators. Values are reported in picomoles. Error bars represent ± SE. Sample size n=6, except for controls (n=16), SADC (n=10), MEADC and HEDC (n=4) and AAPH and ABMP (n=3). *p< 0.01 relative to controls by one-way ANOVA and Dunnett's Multiple Comparison post hoc test.

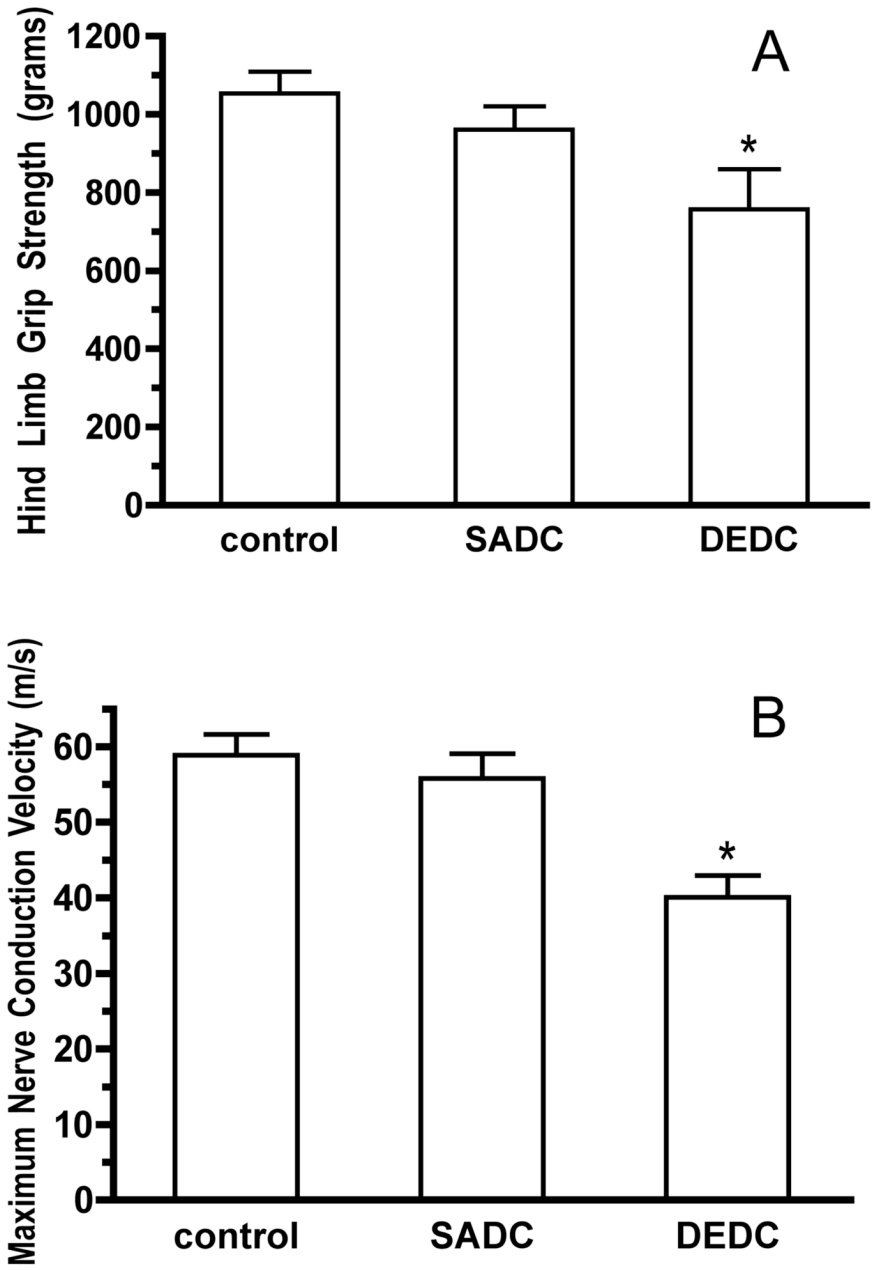

Figure 3.
Neuromuscular function as assessed by hind limb grip strength and NCV. Values for grip strength (A) are reported as mean peak compression (g). Values for NCV (B) are reported as mean velocity (m/s). Error bars represent ± SE, with sample size n=6. *p< 0.01 relative to control and SADC groups by one-way ANOVA and Tukey-Kramer post hoc test.

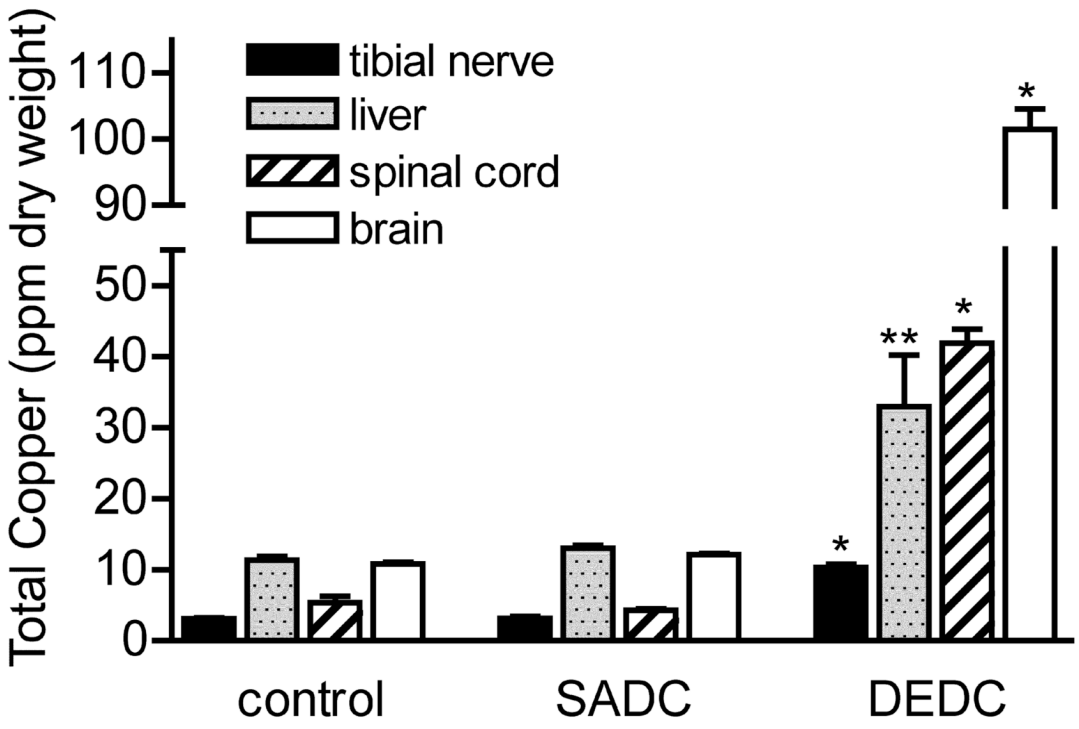

Figure 4.

Total tissue copper levels. Values for brain, spinal cord, tibial nerve, and liver were determined by ICP-MS (n=6) and are reported as mean ppm dry weight of tissue. Error bars represent ± SE. *$p < 0.001$ relative to controls and SADC by One-way ANOVA and Tukey-Kramer post hoc test, ** $p<0.05$ relative to Controls and SADC by one-way ANOVA and Tukey-Kramer post hoc test.

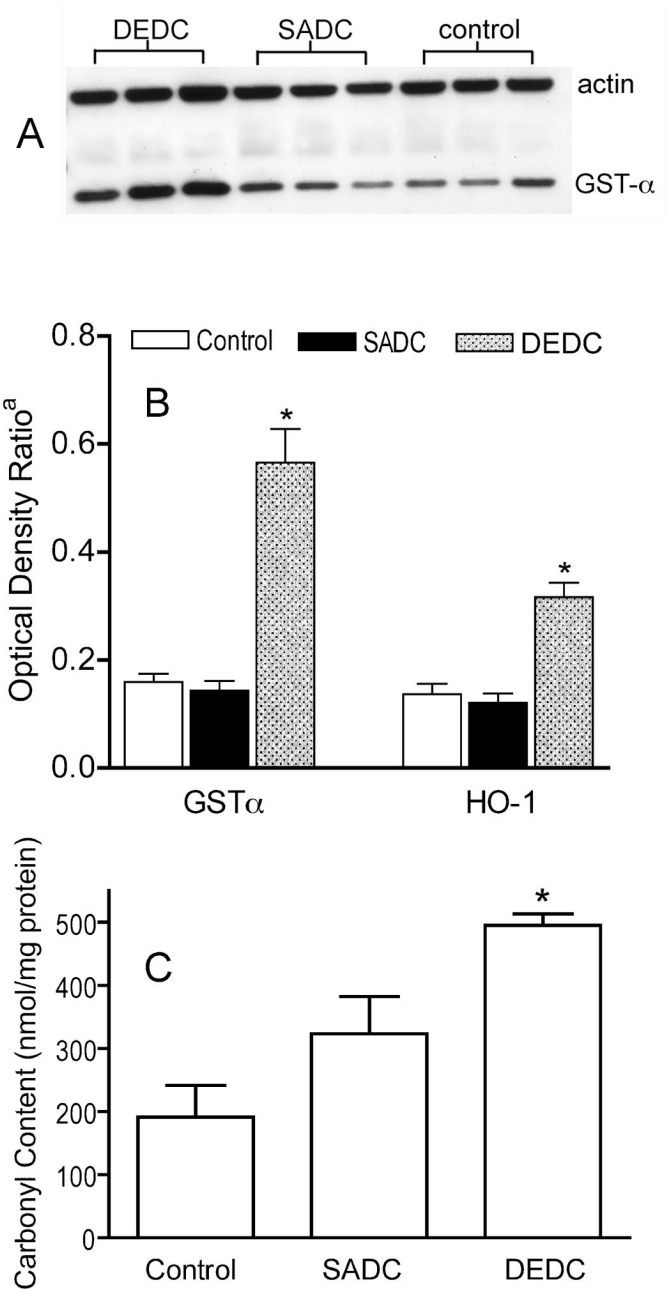

Figure 5.

(A) Representative Western Blot showing relative amounts of GST-α in proteins isolated from sciatic nerves of DEDC, SADC and control animals. (B) Amount of GST-α and HO-1 in sciatic nerve proteins normalized to sciatic nerve actin from DEDC, SADC and control animals as measured by optical density of Western Blots. [a] Optical Density Ratio = OD GST-α or HO-1/ OD actin (n=6, except n=5 for GST-α, SADC group). Error bars represent ± SE. *$p < 0.001$ relative to SADC and controls by one-way ANOVA and Dunnett's Multiple Comparison post hoc test. (C) Total protein carbonyl level in sciatic nerve proteins isolated from Control, SADC and DEDC-exposed rats as determined by slot-blot analysis. Proteins were isolated from sciatic nerves, derivatized with fluoresceinamine, slot blotted to PVDF, and the amount of protein and

protein carbonyls determined by protein staining with densitometry and immunodetection with chemiluminescence, respectively (see Experimental Procedures for details). Values are expressed as mean nmoles fluoresceinamine/mg sciatic nerve protein ± SE (n = 6, except n = 5 for controls). *$p<0.01$ relative to controls, by one-way ANOVA and Dunnett's Multiple Comparison post hoc test.

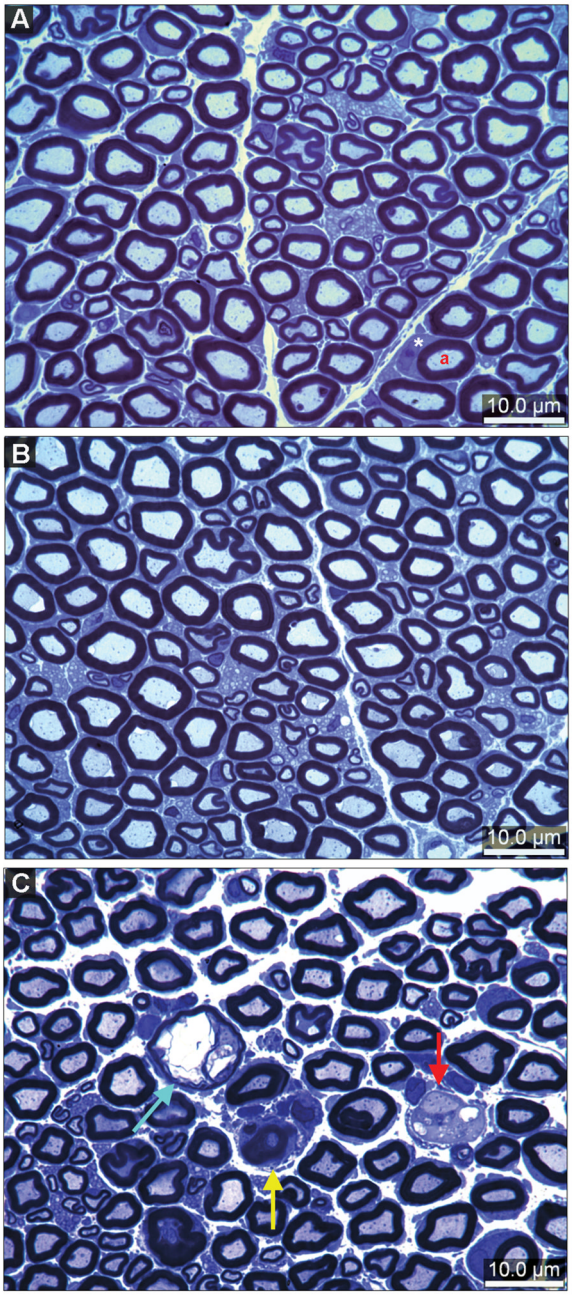

Figure 6.
Morphology of sciatic nerve cross-sections stained with toluidine blue. (A) Cross section obtained from a control rat showing the presence of large and small myelinated axons. The axons (a) are surrounded by normal compact myelin. A Schwann cell has been sectioned through its cytoplasm (*). (B) Cross section of a nerve obtained from a SADC-exposed rat showing normal large and small myelinated axons. (C) Cross section of a sciatic nerve from an animal exposed to DEDC for 8 weeks demonstrating an axon with intramyelinic edema (blue arrow), a demyelinated axon (red arrow) surrounded by Schwann cell cytoplasm, and degenerating axon (yellow arrow).

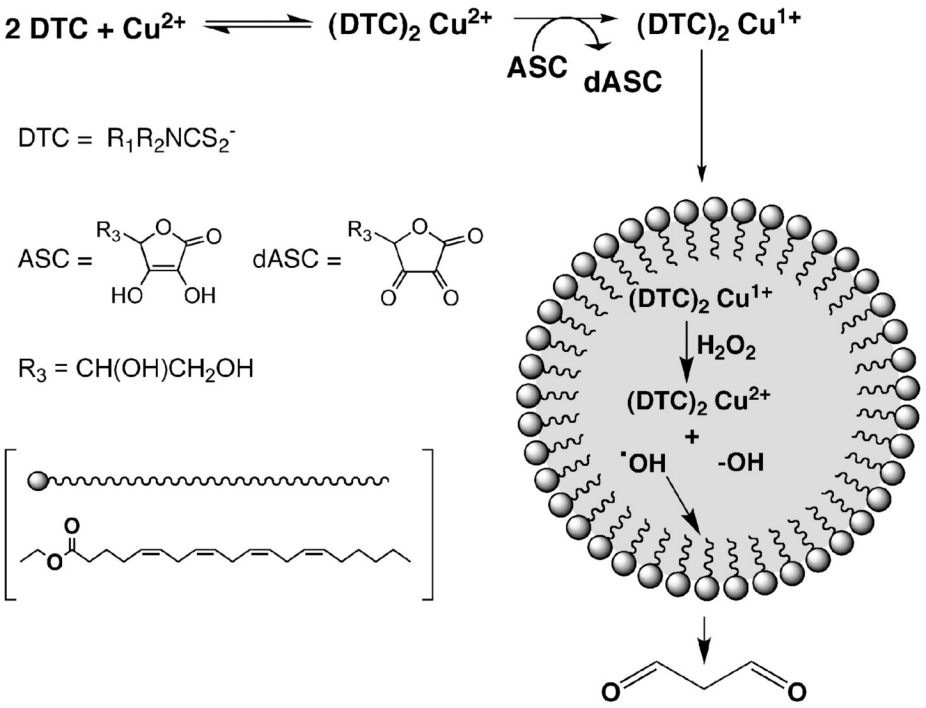

Scheme 1.
Proposed mechanism for dithiocarbamate facilitated generation of MDA by Cu^{2+}.

Table 1

Incidence and Severity of Sciatic Nerve Lesions[a]

Treatment	Degenerated axons		Thin myelin		Demyelination		Intramyelinic edema	
	Incidence[b]	Severity[c]	Incidence[b]	Severity[c]	Incidence[b]	Severity[c]	Incidence[b]	Severity[c,g]
Controls	6/6	2.07 (0.22)	0/6	0 (0)	0/6	0 (0)	0/6	0 (0)
Range		(1.17–2.66)						
SADC[d]	5/5	2.88 (0.13)[e]	0/5	0 (0)	0/5	0 (0)	0/5	0 (0)
Range		(2.55–3.33)						
DEDC	6/6	3.82 (0.18)[e,f]	2/6	0.58 (0.37)	4/6[h]	0.94 (0.35)[e,f]	4/6[h]	1.35 (0.64)
Range		(3.30–4.37)		(0.00–1.73)		(0.00–2.24)		(0.00–4.24)

[a] Slides were scored by a single observer (HLV). One entire sciatic nerve fascicle was examined under light microscopy and lesions totaled then divided by section surface area. n=6 unless otherwise noted.

[b] Number of animals with positive observations/number of animals in treatment group.

[c] Mean of square root of number of axons with lesions divided by mm^2 surface area (SE).

[d] n=5

[e] $p < 0.05$ as compared to Controls by one-way ANOVA, Tukey Kramer post hoc test.

[f] $p < 0.05$ as compared to SADC by one-way ANOVA, Tukey Kramer post hoc test.

[g] $p < 0.05$ between means of groups by ANOVA only.

[h] $p < 0.01$ with respect to incidence between groups by Chi-square and Chi-squared for trend.